Two-time correlations, self-averaging, and an analytically solvable model of phase-ordering dynamics

Chuck Yeung and David Jasnow
Department of Physics and Astronomy, University of Pittsburgh, Pittsburgh, Pennsylvania 15260
(Received 9 April 1990)

We consider a simple model of phase-ordering dynamics with nonconserved order parameter introduced by Ohta, Jasnow, and Kawasaki. We demonstrate that, within this model, any expectation value, including multiple-time-correlation functions, can be obtained. Although the dynamics are very simple and are spatially non-self-averaging only in a trivial sense, much of the seemingly complex behavior seen in simulations of more realistic models is reproduced. The model of Ohta *et al.* also suggests a new type of dynamical universality class that is characterized by the lack of *temporal*, as opposed to spatial, self-averaging. The predictions of this model are found to agree well with numerical experiments.

I. INTRODUCTION

In a typical experiment in phase-ordering dynamics, a system initially in the one-phase regime is rapidly quenched into the two-phase regime. It is now known that the subsequent ordering process involves a single time-dependent length with which all other relevant lengths scale. This length grows asymptotically as a power law in time with the exponent depending crucially on whether the order parameter is, or is not, conserved.[1] More recently, attention has been drawn to correlations between the system at two different times.[2–5] In particular, Roland and Grant have performed an interesting Monte Carlo study of the Ising model with nonconserved order-parameter dynamics.[3] Their results indicate that the growth fluctuations have a noise spectrum of the form $1/\omega^{\beta}$ and that the spin-flip probability distributions display multiscaling behavior.[6] These features were attributed to the (spatial) non-self-averaging nature of the dynamics.[7–10] However, it is often very difficult to determine if numerical results are truly asymptotic or if, on the contrary, the observed behavior is due to the finite times and sizes of the experiment. It is also known that, while the asymptotic dynamical growth exponents of the Ising model and the corresponding coarse-grained description are the same, other features are quite different.[11] Finally, although phase-ordering dynamics is said to be non-self-averaging,[7–10] the precise meaning of this is often unclear.

In order to clarify the situation and explore the interrelations of these results and concepts, we consider a model of phase ordering dynamics with nonconserved order parameter introduced by Ohta, Jasnow, and Kawasaki.[12] As will be shown, the advantage of the Ohta-Jasnow-Kawasaki (OJK) model is that any expectation value can, in principle, be calculated, and the asymptotic scaling behavior can be obtained unambiguously. The dynamics are extremely simple and are (spatially) non-self-averaging only in a trivial sense. However, many interesting features, including a $1/\omega^{\beta}$-type power spectrum are observed. More importantly, we find that the OJK model suggests the possibility of a new type of *dynamical universality class*, which is characterized by the lack of *temporal*, as opposed to spatial, self-averaging.

Simple multiple-time[4] and finite-size[7,13] scaling arguments are used to extend some of the results to phase-ordering dynamics in general. We find that, in general, the dynamical behavior of statistical uncertainties depend on the (spatial) self-averaging exponent. The scaling forms for the autocorrelation functions and power spectra are also found to depend on the (spatial) self-averaging exponent.

The OJK model is one of the few analytically tractable models in phase-ordering dynamics. In light of the model's surprising predictions, a second purpose of this paper is to test the ability of the OJK model to describe the scaling behavior in more realistic models of the phase-ordering process. Previous tests of the OJK model have not been very stringent. To this end, we have performed simulations of the cell dynamical system[14] corresponding to the phase-ordering dynamics with a nonconserved order parameter. The numerical simulations provide a test of the general scaling results noted above and of the universality of the effects observed by of Roland and Grant.[3] Considering the simplicity of the OJK model, the numerical simulations are found to agree remarkably well with the predictions of the OJK model. In particular, as predicted by the OJK model, the dynamics are spatially non-self-averaging only in a trivial sense but some variables are *temporally* non-self-averaging.

The organization of the remainder of this paper is as follows. In Sec. II various definitions and terminology are introduced. In Sec. III the OJK model is described, while in Sec. IV results of specific calculations are given. Section V extends some of the results of the OJK model to more general systems exhibiting dynamical scaling. Section VI describes the numerical simulations and compares the results with the predictions of the OJK model.

Section VII is a discussion and summary. The details of the calculations described in Sec. IV are shown in the Appendix.

II. DEFINITIONS

We start with more precise definitions of the terminology used in this paper. Consider performing an expermental measurement of an intensive quantity g. There are three ways one might attempt to decrease the statistical uncertainty

$$\langle \delta g^2 \rangle^{1/2} = \langle (g - \langle g \rangle)^2 \rangle^{1/2} .$$

The $\langle\ \rangle$ indicates an ensemble average. The first way is to increase the number of independent trials n. The uncertainty always decreases as $1/\sqrt{n}$. The second way is to increase the volume of the system L^d, where L is the linear system size and d is the spatial dimensionality. In general, the uncertainty in g will decrease as $L^{-\Delta/2}$. Using the terminology of Milchev *et al.*,[7] we will refer to this as *spatial* self-averaging and Δ as the spatial self-averaging exponent. If $\Delta = d$, g is said to be (spatially) a *strongly* self-averaging quantity, if $0 < \Delta < d$, g is said to be (spatially) a *weakly* self-averaging quantity, and if $\Delta = 0$, g is said to be (spatially) a *non-self-averaging* quantity. Note, however, that it is the *combination* of the physical observable *and* the dynamics that has, or does not have, the property of being spatially self-averaging, not the quantity nor dynamics alone. For example, as noted by Milchev *et al.*, the magnetic susceptibility χ obtained from the fluctuation dissipation theorem, $\chi \propto L^d \langle (\delta m)^2 \rangle$, where m is the magnetization density, is a spatially non-self-averaging quantity even for equilibrium systems far from any critical point. Therefore, the lack of (spatial) self-averaging is not, in itself, a sign of "complicated" dynamics.

Hence, to generalize the observation of Milchev *et al.*, we note the following sufficient conditions for obtaining a non-self-averaging quantity. Let A be the density of a local quantity $O(\mathbf{r})$, namely $A = L^{-d} \int d\mathbf{r}\, O(\mathbf{r})$. Consider $X = f(L^{d/2} \delta A)$, where δA is the fluctuation in A and f is any piecewise continuous function. Then, if $\langle O(\mathbf{r}) O(\mathbf{r}') \rangle$ decays to zero sufficiently fast as $|\mathbf{r} - \mathbf{r}'| \to \infty$ (faster than $|\mathbf{r} - \mathbf{r}'|^{-d}$), the quantity X will be (spatially) non-self-averaging. This conclusion is due to the following considerations. Under the above circumstances, two widely separated regions will be uncorrelated and the central limit theorem shows that A is a Gaussian process. Straightforward analysis reveals that X is (spatially) non-self-averaging. Under these circumstances we refer to the non-self-averaging behavior as "trivial" to distinguish the possibility of non-self-averaging behavior of more significant origins. We will demonstrate that, if a quantity is non-self-averaging in this sense, one can obtain a spatially non-self-averaging observable with as much precision as a strongly self-averaging one.

The third way one might attempt to decrease the uncertainty is to perform longer experiments and take the time average. If the system is ergodic, the uncertainty will decrease as $1/\sqrt{t}$ for large t, where t is the length of the experiment. In a phase-ordering experiment, one is interested in the approach to the stationary state, so the interesting behavior is inherently nonergodic. However, time-independent amplitudes can still be defined.[3] Let $g(t)$ be a time-dependent quantity which behaves asymptotically as $g(t) \sim t^{\beta}$. Dividing by the asymptotic form defines an amplitude with a time-independent expectation value, i.e., $g(t)/t^{\beta}$. We will say g is *temporally* self-averaging if the uncertainty in the corresponding amplitude vanishes in the limit of an infinitely long experiment.

Since we will be interested in a nonstationary system, we must also generalize the usual definitions of correlations for stationary processes. For $\langle g(t) \rangle \neq 0$, we will call

$$\langle \delta g(t)^2 \rangle^{1/2} / \langle g(t) \rangle$$

the "reduced" uncertainty of $g(t)$. We will call

$$\langle \delta g(t_1) \delta g(t_2) \rangle / [\langle g(t_1) \rangle \langle g(t_2) \rangle]$$

the *reduced* autocorrelation function of g.

III. THE OJK MODEL (DESCRIPTION)

The OJK model can be thought of as the simplest model of phase-ordering dynamics with a nonconserved order parameter which includes the following experimentally observed features: (1) The characteristic length scale $R(t)$ (e.g., size of domains) grows as $t^{1/2}$. (2) The order-parameter field $\psi(\mathbf{r}, t)$ is at one of the bulk equilibrium values $\pm\psi_{\text{eq}}$ everywhere except at the interfaces. (3) The interfacial thickness is time independent and, in the scaling regime, is much smaller than $R(t)$.

The main feature of the method of Ohta *et al.* is the determination of the late-stage phase-ordering dynamics through the introduction of a spatially smooth auxiliary field $u(\mathbf{r}, t)$.[12] The u field obeys the diffusion equation. The order-parameter field $\psi(\mathbf{r}, t)$ is then obtained from the u field via a nonlinear mapping

$$\psi(\mathbf{r}, t) = \psi_{\text{eq}} \text{sgn}[u(\mathbf{r}, t)] .$$

More technically, the OJK evolution equation for u can be obtained from the time-dependent Ginzburg-Landau equation (TDGL) for ψ. By assuming that the interfaces are in local equilibrium, one obtains a nonlinear equation for u which is, effectively, the equation of motion for the interfaces.[15] Ohta *et al.* then make a type of mean-field approximation. The effects of nonlinearity are absorbed into a "renormalization" of the coefficients of the linear terms, and a simple diffusion equation is obtained for u.

A weakness in the OJK model is that the u field is not uniquely defined by the physically observable ψ field. To address this question, Oono and Puri[16] made a smooth nonlinear mapping from u to ψ, i.e.,

$$\psi(\mathbf{r}, t) = \psi_{\text{eq}} \eta_{\xi}(u(\mathbf{r}, t)) ,$$

where $\eta_{\xi}(u)$ is a continuous single-valued function of u which converges to the $\text{sgn}(u)$ as $\xi \to 0$. ξ can be interpreted as the interfacial thickness. The explicit effect of nonzero ξ is included by choosing $\eta_{\xi}(u)$ to be the smooth

interfacial profile of characteristic width ξ. In the Oono-Puri extension of the OJK model, the dynamics of the u field are kept linear,

$$\frac{\partial u}{\partial t}=D\nabla^2 u+h(t)u \ , \tag{3.1}$$

where D is an effective diffusion constant (which can be related to the surface tension), and $h(t)=(d+1)/4t$ is chosen so that the interfacial thickness is time independent. However, the only effect of the finite interfacial thickness is a change in the nonlinear mapping $\eta_\xi(u)$ from $\mathrm{sgn}(u)$. It has no effect on the asymptotic scaling behavior which is still governed by an underlying diffusion equation.

By a different method, Kawasaki *et al.*[17] obtained Eq. (3.1) with a different effective diffusion constant, $h(t)=$const and a specific η_ξ. However, Kawasaki *et al.* and Ohta *et al.* arrive at the same asymptotic scaling behavior and, in both cases, the way in which the linear equation for u is obtained from the TDGL equation is not controlled. This is also true of the Oono-Puri extension of the OJK model.

Due to the simplicity of the linear equation underlying the dynamics, any expectation value can, in principle, be calculated. In particular, the OJK model correctly predicts the dynamical scaling behavior and the $t^{1/2}$ growth of the characteristic length scale in agreement with experimental,[18] numerical,[19] and other analytical results.[15] In the scaling regime, the quasistatic scattering function is of the form

$$S_{\mathbf{k}}(t)=\langle \psi_{\mathbf{k}}(t)\psi_{-\mathbf{k}}(t)\rangle = R(t)^d f(q) \ , \tag{3.2}$$

where $\psi_{\mathbf{k}}(t)$ is the Fourier transform of $\psi(\mathbf{r},t)$, $q=R(t)|\mathbf{k}|$, and $f(q)$ is the scaling function. The OJK scaling function is found to be in quantitative agreement with experiments,[12] especially if the Oono-Puri extension is included.[16] As predicted by the OJK model, the experimental scaling function $f(q)$ has a maximum at $q=0$ and, for large q, $f(q)$ seems to approach the Porod's law[20] form $f(q)\sim q^{-(d+1)}$ at long times.[16] However, these features are not a very stringent test of the OJK model. The peak at $q=0$ arises because the ψ field is uncorrelated at large distances. Both this feature and the $t^{1/2}$ growth law is due to the diffusion equation which governs the dynamics of the u field. The Porod's law form at large q is due to the presence of sharp interfaces. In the OJK model this is represented by the sharpness of the nonlinear mapping η_ξ. Due to the large scatter of the data for $S_{\mathbf{k}}(t)$ at small k, any function $f(q)$ which connects the large- and small-q limits smoothly and monotonically will give reasonable agreement with the experimental results.

Independently of its alleged origins in the TDGL equation, the OJK model can be considered to be the simplest possible model of the phase-ordering process. Since the asymptotic behavior of the OJK model can be obtained unambiguously, the OJK model is a useful tool in determining if an observed effect is merely a consequence of scaling or is due to some more complicated feature of the dynamics. It is also instructive to test the validity of the OJK model against more realistic models of phase-ordering dynamics, for example, the TDGL equation itself. In particular, knowing the failures of the OJK model will be useful in obtaining insight into features that are needed in the construction of more realistic models, which, one hopes, remain tractable.

IV. THE OJK MODEL (CALCULATIONS)

To specify completely the OJK model one must specify the initial state $u(\mathbf{r},t=0)$ and the exact form of the nonlinear mapping η_ξ. For simplicity, to represent random interfaces, the initial u field is chosen to have a Gaussian distribution with zero mean and no spatial correlation. This reduces the calculation of expectation values to a series of Gaussian integrals. The detailed form of η_ξ will have no effect on the asymptotic scaling behavior, so we follow Oono and Puri and choose η_ξ such that $d\eta_\xi(u)/du$ is a Gaussian of width ξ. This choice of η_ξ simplifies the Gaussian integrals.

Oono and Puri calculated the equal-time two-point correlation function for the order parameter ψ. An extension of their calculation gives the two-time two-point correlation function

$$\langle \psi(\mathbf{r}_1,t_1)\psi(\mathbf{r}_2,t_2)\rangle \ .$$

The details are shown in the Appendix. The general two-point correlation function is

$$\langle \psi_1\psi_2\rangle = \arcsin\left[\beta_1\beta_2\gamma_{12}\exp\left[\frac{-|r_1-r_2|^2}{l_1^2+l_2^2}\right]\right] , \tag{4.1}$$

where $\psi_i=\psi(\mathbf{r}_i,t_i)$, $l_i=(4Dt_i)^{1/2}$ is the time-dependent diffusion length, and

$$\gamma_{ij}=\left[\frac{2l_il_j}{l_i^2+l_j^2}\right]^{d/2} , \qquad \beta_i=[1+(\xi/l_i)^2]^{-1/2} \ . \tag{4.2}$$

Here β_i contains the corrections due to the finite interfacial thickness. To simplify the notation, we set $\psi_{\mathrm{eq}}=1$. The results of Ohta *et al.* are recovered in the limit ξ/l_i, $\xi/l_j\to 0$ ($\beta_i,\beta_j=1$). Note that, in general, $\gamma_{ii}=1$, γ_{ij} is symmetric ($\gamma_{ij}=\gamma_{ji}$) and $\gamma_{ij}\to 0$ as either $l_i/l_j\to 0$ or $l_i/l_j\to\infty$.

To study the consequences of spatial self-averaging, we will consider two commonly used definitions of the characteristic length scale $R(t)$. The order-parameter length scale is

$$R_m(t)^d=L^d|m(t)|^2 \ , \tag{4.3}$$

where $m(t)=L^{-d}\int d\mathbf{r}\,\psi(\mathbf{r},t)$ is the order-parameter density. The second length scale is the inverse area density

$$R_a(t)=1/a(t) \ , \tag{4.4}$$

where

$$a(t)=(1/L^d)\int d\mathbf{r}|\nabla\psi(\mathbf{r},t)|\delta(\psi(\mathbf{r},t))$$

is the interfacial area density. The two definitions of

$R(t)$ behave the same way asymptotically, but, within the OJK model, $R_a(t)$ is spatially strongly self-averaging while $R_m(t)$ is spatially non-self-averaging. However, as we will demonstrate, both $R_m(t)$ and $R_a(t)$ are *temporally* non-self-averaging.

The strategy is mapped here. The full calculation is given in the Appendix. Two regions separated by much more than the effective diffusion length $(l_1^2+l_2^2)^{1/2}$ are uncorrelated. Restricting the analysis to the scaling regime $[L \gg l(T)]$, both $\{m(t):0<t\leq T\}$ and $\{a(t):0<t\leq T\}$ are sums of independent processes and so are Gaussian processes. The first and second moments of $m(t)$ and $a(t)$ can be calculated in a straightforward manner and completely specify the probability distributions of both $m(t)$ and $a(t)$. From these probability distributions we can calculate all the moments of $R_m(t)$ and $R_a(t)$. This strategy can be used to calculate any correlation function as long as the quantities can be written a functional of u.

We find that the probability distributions of both $R_a(t)$ and $R_m(t)$ display scaling with a single length, i.e.,

$$\langle R(t)^q\rangle \sim t^{q/2} \sim l(t)^q ,$$

in agreement with the kinetic Ising model results of Roland and Grant.[3] The reduced correlation function $C_m(t_1,t_2)$ of $R_m(t)$ is of the form

$$C_m(t_1,t_2)\equiv \frac{\langle \delta R_m(t_1)\delta R_m(t_2)\rangle}{\langle R_m(t_1)\rangle\langle R_m(t_2)\rangle} = \beta_1\beta_2 F_{m,d}(\beta_1\beta_2\gamma_{12}) , \tag{4.5}$$

where γ_{12} and β_i are defined in Eq. (4.2). The exact form of $F_{m,d}(\gamma)$ depends on the spatial dimension d but is independent of the system size L. The reduced uncertainty $[C_m(t,t)]^{1/2}$ is therefore independent of L making $R_m(t)$ a (spatially) non-self-averaging quantity. Since the system is uncorrelated at large spatial separations, the central limit theorem applies and $R_m(t)$ is spatially non-self-averaging in the trivial sense.

The reduced correlation of $R_a(t)$ is of the form

$$C_a(t_1,t_2)=\left[\frac{l_1 l_2}{L^2}\right]^{d/2} F_{a,d}(\gamma_{12}) , \tag{4.6}$$

where $F_{a,d}(\gamma)$ is another L-independent function of γ. Setting $t_1=t_2=t$, we find that $C_a(t,t)$ decreases as $[l(t)/L]^{-d}$, making $R_a(t)$ a (spatially) strong self-averaging quantity.

However, both $R_m(t)$ and $R_a(t)$ are temporally non-self-averaging quantities. Figure 1 shows $C_a(t_1,t_2)$ and $C_m(t_1,t_2)$ for $d=2$. We have taken the scaling limit $\beta_i=1$. The important feature to note is that, for fixed t_1, both C_m and C_a remain finite as $t_2\to\infty$. This is true for any $d\geq 2$. Therefore, the reduced correlations of both $R_m(t)$ and $R_a(t)$ do not vanish as $t_2/t_1\to\infty$ and *within the OJK model* both $R_a(t)$ and $R_m(t)$ are temporally non-self-averaging quantities.

This is a surprising finding and, as far as we know, the possibility that the correlations do not vanish has not been previously considered. We first demonstrate that

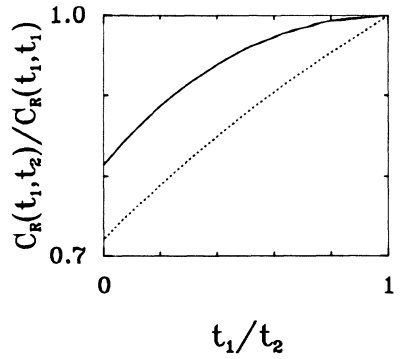

FIG. 1. Linear plot of the reduced autocorrelation functions $C(t_1,t_2)/C(t_1,t_1)$ for $R_m(t)$ and $R_A(t)$ for the OJK model in two dimensions. $C_m(t_1,t_2)$ (solid line) and $C_A(t_1,t_2)$ (dotted line) are plotted vs t_1/t_2. The limit $\xi/l_1,\xi/l_2\to 0$ has been taken. The interesting feature is that both C_m and C_A remain finite as $t_1/t_2\to 0$.

the lack of temporal self-averaging is not an empty feature. Assume that for any single initial condition, asymptotically $R(t)\sim A(t-t_0)^{1/2}+b$. A first guess would be that t_0 and b depend on the initial condition, but that the amplitude A is a property of the asymptotic dynamics, and is therefore independent of the initial condition. Without loss of generality we can assume $\langle t_0\rangle=\langle b\rangle=0$. The reduced correlation of $R(t)$ is then

$$\frac{\langle \delta R(t_1)R(t_2)\rangle}{\langle R(t_1)\rangle\langle R(t_2)\rangle} = \frac{\langle t_0^2\rangle}{4t_1t_2}+\frac{\langle b^2\rangle}{At_1^{1/2}At_2^{1/2}} + \frac{\langle t_0 b\rangle}{2t_1At_2^{1/2}}+\frac{\langle t_0 b\rangle}{2t_2At_1^{1/2}} , \tag{4.7}$$

The reduced correlation thus vanishes for fixed t_1 as $t_2\to\infty$. Therefore, in order for $R(t)$ to be a temporally non-self-averaging quantity, the asymptotic amplitude A must depend on the initial condition and is, hence a statistical quantity.

In order to compare the OJK model to the kinetic Ising model simulations of Roland and Grant, we have calculated the "power spectrum" for the reduced quantities $R_m(t)$ and $R_a(t)$. The power spectrum is defined as

$$\hat{S}_g(\omega)=\lim_{T\to\infty}\hat{S}_{g,T}(\omega) = \lim_{T\to\infty}\frac{1}{T}\int_0^T dt_2\int_0^T dt_1 C_g(t_1,t_2)e^{i\omega(t_1-t_2)} , \tag{4.8}$$

where C_g is the reduced correlation function for the quantity g. $\hat{S}_{g,T}(\omega)$ will exist for any finite T, but, if the process is not stationary, there is no reason to expect $\hat{S}_g(\omega)$ to exist, i.e., it may be zero of infinite. We numerically integrated $\hat{S}_{g,T}(\omega)$ for both $R_a(t)$ and $R_m(t)$. $\hat{S}_{g,T}\sim 1/\omega^2$ for the entire regime investigated (about four decades in ω and eight decades in $\hat{S}_{g,T}$).

This result differs from that of Roland and Grant for the two-dimensional kinetic Ising model. They found that the Fourier transform behaves as approximately $1/\omega^{0.9}$. However, it should be noted that although the

quantity calculated by Roland and Grant is the same as (4.8) for $T\to\infty$, the two definitions may be different for finite T. Roland and Grant first averaged over t_1+t_2 and then calculated the Fourier transform of the averaged quantity with respect to the time difference t_1-t_2.[21]

One can also consider the Fourier transform of the relative correlation function at fixed t_1,

$$\mathrm{Re}\int_{t_1}^{\infty} dt_2 e^{i\omega(t_1-t_2)} C_g(t_1,t_2) \ . \tag{4.9}$$

For a stationary variable this is equivalent to the power spectrum, but this is not true for nonstationary quantities. In order to determine the small ω behavior of the Fourier transform, one must determine the large t_2/t_1 behavior of the correlation function. As shown in the Appendix, $C_a(t_1,t_2)$ decays toward its nonzero asymptotic value as (t_1/t_2) for $d\geq 2$. Therefore, for small ω, the Fourier transform of $C_a(t_1,t_2)$ (for fixed t_1) behaves as $1/\ln\omega$ for $d\geq 2$. $C_m(t_1,t_2)$ decays toward its asymptotic value as $\gamma_{12}^2\sim(t_1/t_2)^{d/2}$. For small ω, the Fourier transform of $C_m(t_1,t_2)\sim 1/\ln\omega$ for $d=2$, but, for $d>2$, $C_m(t_1,t_2)\sim c_0-\omega^{(d-2)/2}$, where c_0 is a constant.

V. GENERAL SCALING RESULTS

In this section, we will extend some of the specific results of the OJK model to dynamical scaling behavior in general. Let L be the system size and ξ be a microscopic length scale. For example, in phase-ordering dynamics (with scalar order parameter), ξ is the interfacial thickness. Let the time-dependent characteristic length scale $R(t)$ grow as t^{α}, and let the scaling variable $g(t)$ have dimensions of L^{x}. The finite-size scaling hypothesis for the probability distribution of g takes the form

$$P(g,t,L,\xi)=g^{-1}Q(gL^{-x},R(t)/L,\xi/L) \ , \tag{5.1}$$

where Q is a dimensionless function only of the dimensionless ratios, gL^{-x}, $R(t)/L$, and ξ/L.

Assme that, in the thermodynamic limit, all the moments $\langle g(t)^q\rangle$ are finite (for finite t). Furthermore, assume that, at fixed $R(t)/L$, the limit $\xi/L\to 0$ is nonsingular. This guarantees that the integrated probability is finite in the thermodynamic limit (at fixed R/L). These two assumptions are often, but not always, valid.[22]

Taking the limit $\xi/L\to\infty$, the moments of g are

$$\begin{aligned}\langle g(t)^q\rangle &= L^{qx}\int d\tilde{g}\,\tilde{g}^{q-1}Q(\tilde{g},R(t)/L,0)\\ &= L^{qx}F_{g,q}(R(t)/L)\\ &\sim R(t)^{qx}\sim t^{qx\alpha} \ ,\end{aligned} \tag{5.2}$$

where $\tilde{g}=gL^{-x}$. This follows from the requirement that the thermodynamic limit exists. Together the two assumptions require that $g(t)$ displays scaling with a single length scale.

Consider the one-time reduced correlation function of the scaling variable g. Using Eq. (5.2), $C_g(t,t)$ is of the form

$$C_g(t,t)=\frac{F_{g,2}(R(t)/L)}{F_{g,1}(R(t)/L)^2}-1 \ . \tag{5.3}$$

The reduced correlation is a function only of $R(t)/L$, and therefore the uncertainty in g is also a function of $R(t)/L$ only. If the uncertainty in g decreases as $L^{-\Delta/2}$, then Eq. (5.3) requires the uncertainty will grow as $R(t)^{\Delta/2}$.

This has practical implications. It is obviously important to be able to determine whether a variable is, or is not, spatially self-averaging. However, it is often very difficult to obtain an accurate value for the self-averaging exponent Δ. The standard method would be to investigate the decrease of the uncertainty as a function of the system size L, but this requires that measurements be made for a sufficient range of L. It is necessary to average over many configurations at each L to obtain the reduced uncertainty, so practically one is limited to making measurements at only a few values of L. Furthermore, very small L cannot be used since other types of finite-size effects (such as edge effects) may become important. This makes it quite difficult to obtain an accurate value for Δ. Relation (5.3) gives an alternative method to determine Δ. One can fix L and determine Δ by studying the *growth* in the reduced uncertainty with t. The extra effort required is minimal as one can measure Δ using the same experiments used to study the dynamical scaling behavior of $g(t)$. Given limited computational resources, this method will allow for a more precise estimate for Δ. Examples will be presented in the next section.

If g is a spatially non-self-averaging variable, many independent measurements of g must be made to obtain a precise value of $\langle g\rangle$. However, it may still be possible to obtain $\langle g\rangle$ with as much precision as for a self-averaging variable. The reason is that, if g is non-self-averaging only in a trivial sense, there will be a correlation length l such that the system is uncorrelated over lengths larger than l. Effectively independent subsystems can be created by breaking up the system into subsystems of linear size much larger than l. Measurements of g on different subsystems are effectively independent, thus increasing the precision of the average by increasing the number of trials. Therefore, if one recognizes that a quantity is spatially non-self-averaging only in the trivial sense, one can obtain the non-self-averaging with as much precision as a strongly self-averaging quantity.

We next obtain the scaling form of the power spectrum. Combining finite-size and multiple-time scaling[4] requires that the reduced autocorrelation function is of the form

$$C_g(t_1,t_2,L)=L^{\Delta'}\tilde{F}_g(R(t_1)/L,R(t_2)/L) \ . \tag{5.4}$$

To connect this with Eq. (5.3), we rewrite this as

$$\begin{aligned}C_g(t_1,t_2,L)=L^{\Delta'}&\left[\frac{R(t_1)}{L}\frac{R(t_2)}{L}\right]^{\Delta/2}\\ &\times F_g(R(t_1)/R(t_2),R(t_1)/L) \ .\end{aligned} \tag{5.5}$$

Setting $t_2=t_1$ gives

$$C_g(t_1,t_1,L)=L^{\Delta'}\left[\frac{R(t_1)}{L}\right]^{\Delta}F(1,R(t_1)/L) \ . \tag{5.6}$$

Equation (5.3) requires that this be a function of the ratio

$R(t_1)/L$ only so that $\Delta'=0$. In addition, the self-averaging exponent Δ is defined in the large-L limit so $F_g(y=1,x)$ must approach a constant as $x\to 0$. We will assume that this is true for general y, i.e.,

$$F_g(y,x\to 0)=F_g(y) .$$

The two-time correlation function (in the large-L limit) is then of the form

$$C_g(t_1,t_2,L)=\left[\frac{R(t_1)}{L}\frac{R(t_2)}{L}\right]^{\Delta/2}F_g(R(t_1)/R(t_2)) , \quad (5.7)$$

where, from symmetry considerations, $F(y)=F(1/y)$.

The scaling form of the power spectrum is now easy to obtain. The power spectrum of $g(t)/\langle g(t)\rangle$ is defined in Eq. (4.8),

$$\begin{aligned}\hat{S}_g(\omega)&=\lim_{T\to\infty}\hat{S}_{g,T}(\omega)\\&=\lim_{T\to\infty}\left[\frac{1}{L}\right]^{\Delta}\frac{1}{T}\int_0^T dt_1\int_0^T dt_2 e^{i\omega(t_2-t_1)}(t_1t_2)^{\alpha\Delta/2}F_g(t_1^{\alpha}/t_2^{\alpha})\\&=\lim_{T\to\infty}L^{-\Delta}T^{1+\alpha\Delta}\hat{F}_g(\omega T) ,\end{aligned} \quad (5.8)$$

where $\hat{F}_g(\omega T)$ is a function of ωT only and ωT is a multiple of 2π. We have used $R(t)\sim t^{\alpha}$. If the power spectrum exists, i.e., is nonzero and finite in the limit $T\to\infty$, the power spectrum will be of the form $1/\omega^{1+\alpha\Delta}$. However, since g is not a stationary variable, $\hat{S}_g(\omega)$ does not necessarily exist.

VI. NUMERICAL RESULTS

To test the detailed predictions of the OJK model, we have numerically simulated the phase-ordering dynamics of a nonconserved order parameter. The cell dynamical systems method introduced by Oono and Puri[14] was used. The dynamics are defined by the coupled map

$$\psi_{i,j}(t+1)=A\tanh[\psi_{i,j}(t)]+D[\langle\langle\psi_{i,j}(t)\rangle\rangle-\psi_{i,j}(t)] , \quad (6.1)$$

where i and j are indices defining the position on a two-dimensional square lattice and t, the "time" is the number of updates. Periodic boundary conditions are used. For efficiency, we choose operating parameters $A=1.3$ and $D=0.5$, but, within limits, the specific choice does not matter. $\langle\langle\psi_{i,j}(t)\rangle\rangle$ is the average of ψ over the nearest neighbors of lattice site i,j,

$$\langle\langle\psi_{i,j}(t)\rangle\rangle=\tfrac{1}{4}[\psi_{i+1,j}(t)+\psi_{i-1,j}(t)+\psi_{i,j+1}(t)+\psi_{i,j-1}(t)] . \quad (6.2)$$

The initial state $\psi_{i,j}(0)$ was chosen to have a Gaussian distribution about $\psi=0$ of width 0.05 and no spatial correlation. The cell-dynamical systems method is equivalent to integrating the discrete time-dependent Ginzburg-Landau equations using very large time and space steps.[23]

For the two characteristic lengths $R_m(t)$ and $R_a(t)$, we use discrete versions of (4.3) and (4.4). On a lattice of n^2 cells, the order-parameter length scale is

$$R_m(t)=\frac{1}{n^2}\left[\sum_{i,j}\frac{\psi_{i,j}(t)}{\psi_{\rm eq}}\right]^2 , \quad (6.3)$$

where $\psi_{\rm eq}$ is the fixed point of the mapping $x_{i+1}=A\tanh(x_i)$. The inverse area density is

$$R_a(t)=n^2/N_a(t) , \quad (6.4)$$

where $N_a(t)$ is the number of cells that are on an interface at time t. A cell is defined as being on an interface if $|\psi_{i,j}(t)|\le(0.6)\psi_{\rm eq}$. We have also considered other criteria for determining interface sites. No change in the scaling behavior was observed.

The simulations were carried out on $n\times n$ lattices with $n=192$ (28 initial configurations), $n=256$ (24 initial configurations), and $n=384$ (20 initial configurations). 2896 updates were made from each initial condition. Unless otherwise noted, the quoted results will be from the simulations on the 384^2 lattices.

As expected, the two length scales $R_m(t)$ and $R_a(t)$ grow asymptotically as $t^{1/2}$. For the latest times (2896 updates), both $R_m(t)$ and $R_a(t)$ are about 40 lattice spacings or approximately $\frac{1}{10}$ of the largest lattice. The results for the 384^2 lattice and the 256^2 lattice were consistent with one another, but for $t\ge 2000$, deviate from results for the 192^2 lattice. This was consistent with our observation that finite-size effects were found in the real-space correlation function when the pattern size reaches about $\frac{1}{4}$ of the lattice.

The circularly averaged scattering function is

$$\bar{S}_k(t)=\frac{1}{M(k)}\sum_{k-\Delta k<|\mathbf{k}|\le k+\Delta k}S_{\mathbf{k}}(t) , \quad (6.5)$$

where $\Delta k=2\pi/n$ and $M(k)$ is the number of k modes in the shell $k-\Delta k<|\mathbf{k}|\le k+\Delta k$. Figure 2 shows the scaled circularly averaged scattering function $R(t)^{-2}\bar{S}_k(t)$ versus $q=kR(t)$ along with a fit of the OJK result. $R_a(t)$ is used for the characteristic length. Data

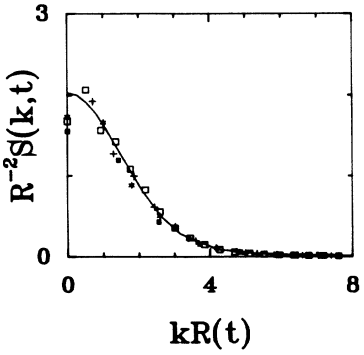

FIG. 2. Linear plot of the scaled scattering function from the simulations on the 384^2 lattice. Data from four times are shown: □ ($t=256$), + ($t=512$), * ($t=1024$), and ● ($t=2048$). The solid line is the two-parameter OJK fit. There is reasonable agreement with the OJK result.

for four times from $t=256$ to 2048 are shown. The OJK scaling function $f(q)$ is obtained by Fourier transforming the real-space correlation function given in Eq. (4.1). The fit contains two adjustable parameters, A and B, defined by $f(0)=B$ and $l(t)=AR(t)$, where $l(t)$ is the diffusion length in the OJK model. The fit parameters are obtained in a very crude manner; a fit is made to one set of data ($t=1024$) and the same values of A and B are used for all the other times. As expected, there is reasonable agreement between the simulation and the prediction of the OJK model.

Figure 3 shows $f(q)$ plotted on a log-log scale along with the OJK result. The behavior at large q can be fit very nicely if the Oono-Puri extension is included. However, even without the Oono-Puri extension, the data are approaching the OJK prediction for large t. In fact, for the latest times, Porod's law $f(q)\sim q^{-3}$ is approximately obeyed over two decades in $f(q)$. This is, to our knowledge, the first time Porod's law has been unambiguously observed in a numerical simulation of the phase-ordering process.

The scattering function does not provide a very stringent test of the predictions of the OJK model. This is especially true for small k since the data show large scatter. Therefore, in order to test whether the OJK model accurately describes the large-scale behavior, one must look directly at the real-space correlation function at large spatial separation rather than the scattering function at small k.

In order to directly compare the simulation results with the predictions of the OJK model, we have eliminated the explicit dependence on the interfacial thickness by applying the mapping $\psi(\mathbf{r},t)=\mathrm{sgn}[\psi(\mathbf{r},t)]$ before calculating $R_m(t)$. This means that, effectively, the interfacial thickness is one lattice spacing. The mapping thus eliminates the extra adjustable parameter introduced in the Oono-Puri extension of OJK model. Note that, although there is no longer any explicit dependence on interfacial thickness, there may still be implicit dependence on the interfacial thickness, i.e., the finite interfacial thickness may lead to a violation of scaling by affecting the dynamics.

Figure 4 shows the circularly averaged scaled real-space correlation function $G(r/R_a(t))$ along with the OJK result given by Eq. (4.1). There is one fit parameter defined by $l(t)=AR_a(t)$. The same value of A was used as in Fig. 2. Data are shown for five times ranging from $t=128$ to 1024. There is excellent agreement with the OJK result. As long as finite-size effects are unimportant ($r\le n/4$), the correlation function decays as predicted by the OJK model, $G(x)\sim\exp(-x^2)$ for large x.

To study the behavior at large temporal separations we consider the two-time correlation function $\langle\psi(\mathbf{r},t_1)\psi(\mathbf{r},t_2)\rangle$. The explicit effect of the interfacial thickness has again been eliminated by applying the sgn map. Figure 5 shows the two-time correlation function for six different t_1 from $t_1=128$ to 1024 and $t_1\le t_2\le 2896$. There is remarkable agreement with the zero-parameter OJK result for all t_1,t_2 shown.

Therefore, somewhat surprisingly, there is excellent agreement between the simulation data and the OJK

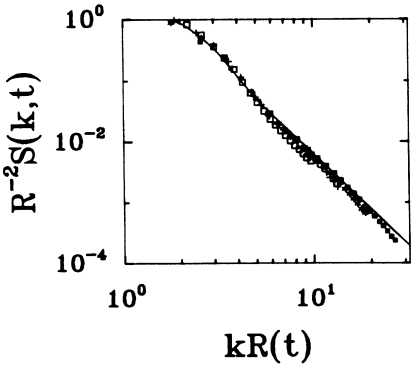

FIG. 3. The same data as Fig. 2 plotted on a log-log scale. For large q the uncertainty is about the same size as the symbols. In the OJK model $f(q)$ obeys Porod's law for large q, $f(q)\sim q^{-3}$. The data from the simulations slowly approaches the OJK form with increasing t. For the largest t, Porod's law is obeyed over two decades in the scattering function.

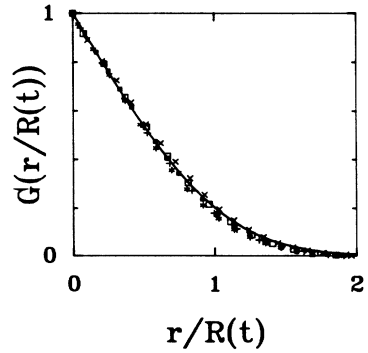

FIG. 4. Plot of the scaled real-space correlation function from the simulations. The uncertainties are smaller than the size of the symbols. The solid line is a one-parameter OJK fit. Data from five times are shown: × ($t=128$), □ ($t=256$), + ($t=512$), * ($t=1024$), and ● ($t=2048$).

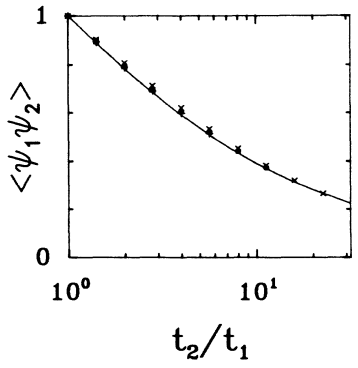

FIG. 5. Linear plot of the two-time correlation function $\langle\psi(\mathbf{r},t_1)\psi(\mathbf{r},t_2)\rangle$ vs t_1/t_2. The uncertainties are smaller than the symbol size. The solid line is the zero-parameter OJK result. Data from four t_1 are shown ($t_1=128-1024$) but the data points fall on top of one another and cannot be differentiated.

correlation functions at both large spatial and temporal separations. Since the ψ field completely defines the system at a given time, this suggests that the asymptotic scaling behavior of most quantities should agree with the OJK predictions. In particular, since the equal-time correlation function $\langle\psi\psi\rangle$ decays rapidly with increasing spatial separation, we expect that the system can be broken up into independent parts and, as noted in Sec. II, the only non-self-averaging quantities will be those that can be related to the fluctuations of a self-averaging quantity.

To test this, Fig. 6 shows the reduced uncertainty squared for $R_m(t)$ and $R_a(t)$ on a log-log scale. The line has a slope of unity. In this case we have divided each 384×384 lattice into four 192×192 lattices, giving 80 configurations. Based on our result for the real-space correlation function, these configurations are effectively independent except, perhaps, at the latest times. As shown in Fig. 6,

$$\langle[\delta R_m(t)]^2\rangle/\langle R_m(t)\rangle^2$$

is time independent to within the statistical uncertainty. Based on the scaling arguments in Sec. V, this implies that $R_m(t)$ is spatially non-self-averaging. On the other hand,

$$\langle[\delta R_a(t)]^2\rangle/\langle R_a(t)\rangle^2$$

increases asymptotically as $t\sim l(t)^2$. Again based on the arguments in Sec. V, this implies that $R_a(t)$ is a (spatially) strongly self-averaging quantity.

Figure 7 shows the normalized reduced correlation function for $R_m(t)$,

$$C_m(t_1,t_2)/C_m(t_1,t_1)$$

along with the zero-parameter OJK result. Data for five different t_1 are shown from $t_1=256$ to 724 and $t_1\le t_2\le2896$. A representative error bar is also shown. There is a systematic deviation from the OJK result, but the deviation violates dynamical scaling and decreases for fixed t_1/t_2 as t_2 is increased. We have also considered the reduced correlation function without eliminating the explicit effects of the finite interfacial thickness, i.e., without applying the sgn mapping. In this case, the deviation from the OJK result increases greatly. Based on these observations we interpret the deviation from the OJK result as being a scaling violation due to nonasymptotic effects, i.e., we expect that, for fixed t_1/t_2, the simulation results will approach the OJK form as t_2 is increased, assuming that L is sufficiently large so that finite-size effects remain unimportant.

Figure 8 shows the normalized reduced correlation function for $R_a(t)$,

$$C_a(t_1,t_2)/C_a(t_1,t_1)$$

along with the zero-parameter OJK result. The agreement with the OJK result is much worse than that for

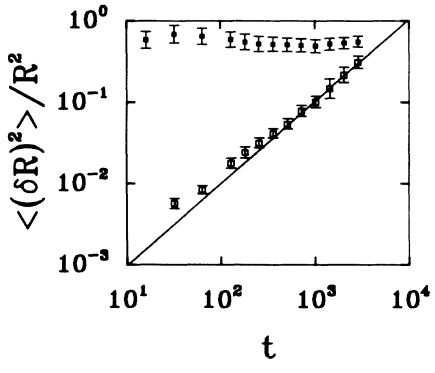

FIG. 6. log-log plot of the reduced uncertainty squared for $R_m(t)$ (solid square) and $R_a(t)$ (open square) vs t. The solid line has a slope of 1. To within the statistical uncertainty, the reduced uncertainty of $R_m(t)$ is time independent while the reduced uncertainty squared of $R_a(t)$ increases asymptotically as $t\sim R(t)^2$.

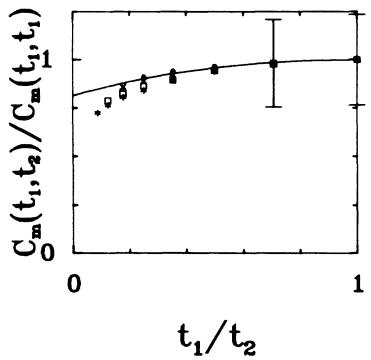

FIG. 7. The normalized reduced correlation function $C_m(t_1,t_2)$ for $R_m(t)$ vs t_1/t_2. Data for four different t_1 along with a representative error bar are shown: * ($t_1=256$), □ ($t_1=362$), + ($t_1=512$), and ● ($t_1=724$). The uncertainties are very large. The solid line is the zero-parameter OJK result.

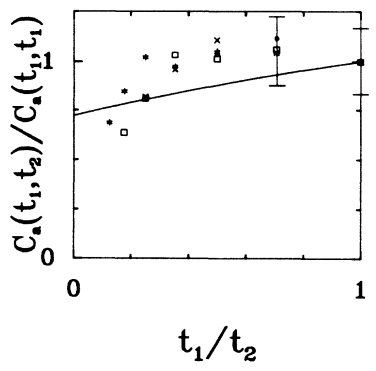

FIG. 8. Same as Fig. 7 but for $R_a(t)$ instead of $R_m(t)$. In this case, the agreement with the zero-parameter OJK result is much worse.

$R_m(t)$ although still within the statistical uncertainty. Therefore, although the numerical results are not inconsistent with the OJK prediction, we cannot rule out that the reduced correlation will decay to zero at large t_2 and that, contrary to the prediction of the OJK model, $R_a(t)$ is temporally self-averaging. In fact, a fit of the tail will give a reasonable fit of the form $(t_1/t_2)^\beta$, where $\beta \ll 1$ over a limited range. Such as result would be consistent with that of Roland and Grant.[3]

There are two points to note. First, due to our criterion for deciding whether or not a point is on an interface, we were unable to eliminate the explicit effect of the interfacial thickness in determining $R_a(t)$. If the sgn mapping were not applied before determining $C_m(t_1,t_2)$, the deviation from the OJK result would be almost as large as that of $C_a(t_1,t_2)$. Without the sgn mapping, the behavior of $C_m(t_1,t_2)$ at small t_1/t_2 would also be very similar to that of $C_a(t_1,t_2)$.

Second, for $t_1=0$, $C_a(t_1,t_2)$ measures the rate at which the dynamical system loses its memory of the initial nonscaling state. This is outside the range of validity of the OJK model in which it is assumed that there are well-defined interfaces at both t_1 and t_2. Therefore, to determine whether a quantity is temporally self-averaging, we need to consider the limit $t_1/t_2 \to 0$ with t_1 fixed and sufficiently large so that well-defined interfaces exist at t_1. In any case, the slow decay of the correlation function is not related to the spatial self-averaging behavior as our results show that $R_a(t)$ is a spatially self-averaging quantity.

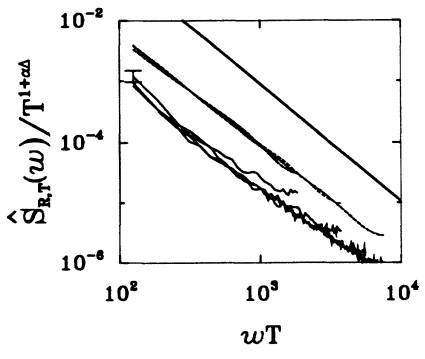

FIG. 9. log-log plot of the scaled power spectrum $T^{1+\alpha\Delta}\hat{S}_{g,T}(\omega T)$ for four different T from $T=600$ to 2400. The lower set of four lines is for R_m while the higher set is for R_a. The thicker solid line is the OJK prediction of $S_{g,T} \sim 1/\omega^2$.

Figure 9 shows the scaled power spectra $\hat{S}_{g,T}(\omega)/T^{1+\alpha\Delta}$ [defined in Eq. (5.8)] for $R_m(t)$ and $R_a(t)$. Data for four different T from $T=600$ to 2400 are shown. The growth exponent α is $\frac{1}{2}$ and the self-averaging exponent Δ is 0 for R_m and Δ is 2 for R_a. The OJK prediction $\hat{S} \sim \omega^{-2}$ is also shown. The scaled power spectrum seems to obey the scaling form (5.8) and behaves as $1/\omega^\beta$ in both cases, with β approximately 2. There is a deviation from the $1/\omega^\beta$ behavior for large ω, but this seems to be an effect due to finite T. We note that, in this case, the data are from a separate set of simulations of 100 configurations on a 196^2 lattice. Here the explicit dependence on the interfacial thickness has not been removed by applying the sgn mapping.

Our numerical results indicate that there are no correlations on length scales much larger than $R(t)$. The only non-self-averaging quantities are those that can be related to the fluctuations of a self-averaging quantity. This would seem to indicate that the TDGL (and OJK) model is in a different universality class from the kinetic Ising model simulations in which the non-self-averaging behavior is said to imply a more complicated type of dynamics, i.e., the system cannot be broken up into independent parts.[3] However, the evidence is not clear. Ising model studies have shown that $R_m(t)$ is non-self-averaging,[7–10] but this may be due solely to the relation of $R_m(t)$ to the fluctuations of the order-parameter density. It is not a good probe of the relation between the dynamics and the system size. Gawlinski *et al.*[9] studied the behavior of $R_m(t)$ and $R_a(t)$ with increasing L. Although their results are not conclusive, there does not seem to be any systematic trend in the behavior of $R_m(t)$ with increasing L. On the other hand, $R_a(t)$ seems to be approaching a limit as L is increased. Sadiq and Binder[8] also found that the uncertainty in the area density decreases with increasing L which is consistent with $R_a(t)$ being a self-averaging quantity.

Another indication that the phase-ordering dynamics of a nonconserved order parameter is non-self-averaging only in the trivial sense is that the interface equations describing the late-stage dynamics are local.[15] The velocity of a point on the interface depends only on the curvature at that point so that local perturbations do not have an immediate effect on points far away. This is not true if the dynamics conserve the order parameter. In this case, the standard models such as the spin-exchange kinetic Ising model or the Cahn-Hilliard-Cook equation have interactions of finite range, but the interfacial equations of motion describing the late-stage dynamics effectively have interactions of infinite range.[24] The reason for the infinite range of interactions is that, in the scaling regime, information from one section of the interface can diffuse across the bulk much faster than the rate at which the interfaces move.[25] The order parameter in the bulk is well described by the quasistatic approximation and there is,

effectively, communication between widely separated sections of the interface [on length scales much larger than $R(t)$]. Hence, for the conserved order parameter case, there may be some interesting non-self-averaging behavior.

VII. DISCUSSION

To summarize, we have shown that a simple model of phase-ordering dynamics introduced by Ohta *et al.*[12] (the OJK model) seems to correctly predict the scaling behavior of a more sophisticated model, namely the time-dependent Ginzburg-Landau equation. The advantage of the OJK model is that the asymptotic scaling behavior can be obtained analytically. We have made cell-dynamical simulations corresponding to the time-dependent Ginzburg-Landau equation. We find that the scaling behavior found in the simulations agrees surprisingly well with the predictions of the OJK model. In particular, the behavior of the order-parameter correlation function is well described by the OJK model at both large temporal and spatial separations.

The OJK model predicts a new type of dynamical universality class which we characterize by the lack of *temporal* self-averaging. In particular, the two definitions of the time-dependent characteristic length $R(t)$ that we have investigated are both, within the OJK model, temporally non-self-averaging. We find that the results of the simulation, though not conclusive, seems to agree with the OJK predictions on this matter.

The lack of temporal self-averaging may explain some puzzling empirical observations. It is often found that if a quantity $g(t)$ grows as t^{β}, an accurate value of the exponent β can be obtained even though there is a very large uncertainty in the amplitude. If $g(t)$ is temporally non-self-averaging, the asymptotic value of the amplitude $g(t)/t^{\beta}$ would depend on the initial condition, so the large scatter in the amplitude would not necessarily affect the accuracy of the value of the dynamical exponent. Furukawa has also considered the two-time correlation of the chemical potential in spinodal decomposition.[4] By making a log-log plot of the chemical potential correlation function, it was observed that the two-time correlation function decayed as a power law in the ratio of times in three spatial dimensions but could not be fit to a straight line in two spatial dimensions. A possible explanation is that, in two dimensions, the chemical potential is not temporally self-averaging.

It would also be interesting to determine if the lack of temporal self-averaging (at least for a class of variables) is a property of phase-ordering dynamics in general. For example, is it a property of the zero-temperature fixed point, which is said to describe phase-ordering dynamics?[26] It may also be possible that these results are not robust to the addition of noise or changes in the initial condition. Adding spatial correlation to the initial condition or adding noise to the dynamics does not seem to effect the scaled scattering function or the asymptotic growth exponent,[27] but it is not known if there will be some effect on two-time correlation functions.

The OJK model was also used to investigate the relation between spatial self-averaging and observed features such as a $1/\omega^{\beta}$ power spectrum. General scaling arguments were used to find a more practical technique to determine the self-averaging exponent of a scaling variable. The scaling form of the power spectrum was also found to depend on the self-averaging exponent. However, we found *no connection* between a $1/\omega^{\beta}$ power spectrum and spatial self-averaging behavior. Our numerical results demonstrate that the order-parameter correlation function decays rapidly for large spatial separations. This indicates, in agreement with the OJK model and the numerical results for R_a and R_m, that the dynamics are spatially non-self-averaging only in a trivial sense. We argued that this interpretation is consistent with previous simulations of the kinetic Ising model without order-parameter conservation.

ACKNOWLEDGMENTS

We would like to thank T. R. Rogers, W. I. Goldburg, and M. Grant for very helpful conversations. We gratefully acknowledge the Pittsburgh Supercomputer Center for a generous grant of computing time. This work was supported by the National Science Foundation through the Division of Materials Research Grant No. DMR86-13030 and DMR89-14621.

APPENDIX

The OJK calculations are explicitly shown in this appendix. The calculations are based on an extension of a method used by Oono and Puri.[16]

Let

$$\phi(\mathbf{r},t)\equiv\psi(\mathbf{r},t)/\psi_{\rm eq}+1=\eta_{\xi}(u(\mathbf{r},t))+1\ ,$$

where $\psi(\mathbf{r},t)$ is the order parameter and $\eta_{\xi}(u)$ is a single-valued function of u which converges to $\mathrm{sgn}(u)$ in the limit $\xi\to 0$. $u(\mathbf{r},t)$ is the auxiliary field obeying Eq. (3.1) and $u(\mathbf{r},0)$ is assumed to have a Gaussian distribution with zero mean and no spatial correlation. ϕ can be written as

$$\phi(\mathbf{r},t)=\int_{-\infty}^{\infty} du\ \theta(u(\mathbf{r},t)-u)\eta'_{\xi}(u)\ , \tag{A1}$$

where $\theta(u)$ is the step function and $\eta'_{\xi}(u)=d\eta_{\xi}/du$. Writing Eq. (A1) in terms of Fourier transforms

$$\phi(\mathbf{r},t)=\lim_{\epsilon\to 0^{+}}\frac{1}{2\pi}\int dv\ e^{ivu(\mathbf{r}_1,t_1)}\frac{i}{v-i\epsilon}\hat{\eta}'_{\xi}(v)\ , \tag{A2}$$

where $\hat{\eta}'_{\xi}$ is the Fourier transform of η'_{ξ}. We follow Oono and Puri and choose

$$\eta'_{\xi}(u)=\frac{2}{(2\pi\xi^2)^{1/2}}\exp\left[\frac{-u^2}{2\xi^2}\right]\ . \tag{A3}$$

This choice of η_{ξ} greatly simplifies the calculation but does not effect the asymptotic scaling behavior.

Since $u(\mathbf{r},t)$ is a Gaussian random variable, it is straightforward to average over the initial conditions. The order-parameter correlation function becomes (for a critical quench)

$$\langle \phi_1 \phi_2 \rangle = - \left[\frac{1}{\pi} \right]^2 \lim_{\epsilon \to 0} \int \frac{dv_1}{v_1 - i\epsilon} \int \frac{dv_2}{v_2 - i\epsilon} \exp[-\tfrac{1}{2}(v_1^2 + v_2^2 + 2\alpha_{12} v_1 v_2)] \ , \tag{A4}$$

where

$$\alpha_{12} \equiv \frac{\langle u_1 u_2 \rangle}{(\xi^2 + \langle u_1^2 \rangle)^{1/2} (\xi^2 + \langle u_2^2 \rangle)^{1/2}} = \beta_1 \beta_2 \gamma_{12} \exp \left[\frac{-|\mathbf{r}_1 - \mathbf{r}_2|^2}{l_1^2 + l_2^2} \right] \tag{A5}$$

and

$$\gamma_{12} \equiv \left[\frac{2 l_1 l_2}{l_1^2 + l_2^2} \right]^{d/2} , \qquad \beta_i = [1 + (\xi^2 / l_i)^2]^{1/2} \tag{A6}$$

with $l_i = l(t_i) = (4Dt_i)^{1/2}$ and $\langle u_i^2 \rangle = l_i^2$. Performing the integration gives

$$\langle \psi_1 \psi_2 \rangle = \psi_{\rm eq}^2 \arcsin \left[\beta_1 \beta_2 \gamma_{12} \exp \left[\frac{-|\mathbf{r}_1 - \mathbf{r}_2|^2}{l_1^2 + l_2^2} \right] \right] , \tag{A7}$$

which is just Eq. (4.1).

To calculate $\langle R_m(t_1) \rangle$ and $\langle R_m(t_1) R_m(t_2) \rangle$, we need to calculate $\langle m(t) \rangle$ and $\langle m(t_1) m(t_2) \rangle$, where

$$m(t) = L^{-d} \int d\mathbf{r} \, \psi(\mathbf{r}, t) / \psi_{\rm eq} \ .$$

As long as $l(t) \ll L$, $\{ m(t), 0 < t < T \}$ is a Gaussian process and these two moments completely define the probability distribution of m. For simplicity we will only consider a critical quench so $\langle m(t) \rangle = 0$. The two-time correlation function is then

$$\begin{aligned} \langle m(t_1) m(t_2) \rangle &= L^{-2d} \int d\mathbf{r}_1 \int d\mathbf{r}_2 \langle \psi(\mathbf{r}_1, t_1) \psi(\mathbf{r}, t_2) \rangle \\ &= L^{-d} \Omega_d (l_1^2 + l_2^2)^{d/2} \int dx \, x^{d-1} \arcsin(\beta_1 \beta_2 \gamma_{12} e^{-x^2}) \\ &= \left[\frac{l_1 l_2}{L^2} \right]^{d/2} \beta_1 \beta_2 \Omega_d 2^{(d-2)/2} K_d \kappa_d(\beta_1 \beta_2 \gamma_{12}) \ , \end{aligned} \tag{A8}$$

where Ω_d is the surface area of a d-dimensional unit sphere, K_d is a dimensional constant,

$$K_d = \int_0^1 du \frac{\arcsin u}{u} \left[\ln \frac{1}{u} \right]^{(d-2)/2} \tag{A9}$$

and

$$\kappa_d(\gamma) = \frac{1}{K_d \gamma} \int_0^\gamma du \frac{\arcsin u}{u} \left[\ln \frac{\gamma}{u} \right]^{(d-2)/2} , \tag{A10}$$

so that $\kappa_d(1) = 1$. κ_d simplifies, for $d = 2$, to

$$\kappa_2(\gamma) = \frac{2}{\pi \ln 2\gamma} \frac{1}{\gamma} \int_0^\gamma du \frac{\arcsin u}{u} \tag{A11}$$

with $\kappa_2(0) = 2/(\pi \ln 2)$. Note that, for any $d \geq 2$, $\kappa_d(0) > 0$.

The joint probability distribution for $m(t_1)$ and $m(t_2)$ is

$$\begin{aligned} P(m_1, t_1; m_2, t_2) = \frac{1}{2\pi} \{ \langle m_1^2 \rangle \langle m_2^2 \rangle [1 - \kappa_d(\gamma)^2] \}^{-1/2} \\ \times \exp \left[-\frac{1}{2} \left[\frac{1}{1 - \kappa_d(\gamma)^2} \right] \left[\frac{m_1^2}{\langle m_1^2 \rangle} + \frac{m_2^2}{\langle m_2^2 \rangle} - \frac{2\kappa_d(\gamma) m_1 m_2}{\langle m_1^2 \rangle \langle m_2^2 \rangle} \right] \right] , \end{aligned} \tag{A12}$$

where $\langle m_i^2\rangle=\langle m(t_i)^2\rangle$ and $\gamma=\beta_1\beta_2\gamma_{ij}$. The expectation values for $R_m(t)$ are

$$\langle R_m(t)^q\rangle=2L^q\int_0^\infty dm\, m^{2q/d}P(m,t)\sim l(t)^q \tag{A13}$$

and

$$\langle R_m(t_1)R_m(t_2)\rangle=2L^2\int_0^\infty dm_1\int_0^\infty dm_2(m_1m_2)^{2/d}\times P(m_1,t_1;m_2,t_2)+P(m_1,t_1;-m_2,t_2)\ . \tag{A14}$$

Combining the previous two expressions gives the reduced autocorrelation function for R_m. For $d=2$ the reduced autocorrelation function $C_m(t_1,t_2)$ becomes

$$\frac{\langle\delta R_m(t_1)\delta R_m(t_2)\rangle}{\langle R_m(t_1)\rangle\langle R_m(t_2)\rangle}[1-\kappa_2(\gamma)^2]^{1/2}-1+\kappa_2(\gamma)\arcsin[\kappa_2(\gamma)]\ . \tag{A15}$$

For general d the reduced autocorrelation function is of the form $c_{0,d}+c_{2,d}\gamma^2+\mathcal{O}(\gamma^4)$ for small γ, where the dimensional constants $c_{0,d}$, $c_{2,d}$ are positive. In the scaling regime β_i is unity and the reduced correlation $C_m(t_1,t_2)$ behaves as $(t_1/t_2)^{d/2}$ for small t_1/t_2.

The autocorrelation for $R_a(t)$ can be calculated the same way. In this case the probability distribution for the area density is needed with

$$a(t)=\frac{1}{L^d}\int d\mathbf{r}|\nabla u(\mathbf{r},t)|\delta(u(\mathbf{r},t))\ . \tag{A16}$$

Introducing the Fourier transform,

$$\langle a(t)\rangle=\left\langle\frac{1}{2\pi}\int dv\, e^{ivu(\mathbf{r},t)}\right\rangle=[2\pi l(t)^2]^{-1/2}\ . \tag{A17}$$

The $|\nabla u|$ factor has not been included since $h(t)$ in Eq. (2.1) is chosen to keep $|\nabla u|$ constant near $u=0$. The reduced autocorrelation for $a(t)$ is

$$\frac{\langle\delta a(t_1)\delta a(t_2)\rangle}{\langle a(t_1)\rangle\langle a(t_2)\rangle}=\frac{1}{L^d}\left[\frac{l_1^2+l_2^2}{2}\right]^{d/2}\int dx\left[\frac{1}{(1-\gamma_{12}^2e^{-x^2})^{1/2}}-1\right],$$
$$=\left[\frac{l_1l_2}{L^2}\right]^{d/2}\Omega_d\frac{1}{\gamma_{12}}\int_0^{\gamma_{12}^2}du\frac{1-\sqrt{1-u}}{u\sqrt{1-u}}\left[\ln\frac{u}{\gamma_{12}^2}\right]^{(d-2)/2}\ . \tag{A18}$$

The definition of $a(t)$ does not depend on the mapping η_ξ so the reduced autocorrelation function is independent of β_i.

The reduced autocorrelation of $R_a(t)$ is the same as that of $a(t)$. For $d=2$, the analysis of Eq. (A18) gives

$$\frac{\langle\delta R_a(t_1)\delta R_a(t_2)\rangle}{\langle R_a(t_1)\rangle\langle R_a(t_2)\rangle}=\left[\frac{l_1l_2}{L^2}\right]^{d/2}\frac{4\pi}{\gamma_{12}}\ln\frac{2[1-(1-\gamma_{12}^2)^{1/2}]}{\gamma_{12}^2}\ .$$

For general dimensions, the reduced autocorrelation function behaves as

$$(l_1l_2)^{d/2}[c_{1,a}\gamma_{12}+c_{3,d}\gamma_{12}^3+\mathcal{O}(\gamma_{12}^5)]$$

for small γ. $c_{1,d}$ and $c_{3,d}$ are dimensionally dependent constants. For fixed t_1 and small t_1/t_2, the reduced correlation of R_a behaves as

$$c'_{1,d}+c'_{3,d}(t_1/t_2)+\mathcal{O}(t_1/t_2)^2\ .$$

The techniques used above can be generalized to allow calculations of expectation values of other observables. In principle, all that is necessary is that the observable can be written as a function of an intensive variable. Denote this intensive variable as $g(t)$. The u field completely defines the configuration, so if $g(t)$ is a physically meaningful quantity, it can be written as a functional of the u field. If u is a Gaussian random variable, the expectation values can then be calculated by first raising $u(\mathbf{r},t)$ to the exponent using relation (A2). It is then straightforward to average over the initial conditions and to calculate the first and second moments of $g(t)$. Since $g(t)$ is also a Gaussian process, these moments completely define the probability distribution of $g(t)$. In practice, the calculations may be technically difficult but, if necessary, can be performed numerically.

[1]For reviews, see J. D. Gunton, M. san Miguel, and P. S. Sahni, in *Phase Transitions and Critical Phenomena*, edited by C. Domb and J. L. Lebowitz (Academic, London, 1983), Vol. 8; H. Furukawa, Adv. Phys. **34**, 703 (1985); K. Binder, Physica A **140**, 35 (1986).

[2]C. Billotet and K. Binder, Physica A **103**, 99 (1980).

[3]C. Roland and M. Grant, Phys. Rev. Lett. **63**, 551 (1989).

[4]H. Furukawa, J. Phys. Soc. Jpn. **58**, 216 (1989); Phys. Rev. B **40**, 2341 (1989).

[5]T. J. Newman and A. J. Bray, J. Phys. A **23**, L279 (1990); A. J. Bray, *ibid.* **22**, L67 (1989); T. J. Newman, A. J. Bray, and M. A. Moore, Phys. Rev. B **42**, 4514 (1990).

[6]T. C. Halsey, M. H. Jensen, L. P. Kadanoff, I. Procaccia, and B. I. Schraiman, Phys. Rev. A **33**, 1141 (1986).
[7]A. Milchev, K. Binder, and D. W. Heermann, Z. Phys. B **63**, 521 (1986).
[8]A. Sadiq and K. Binder, J. Stat. Phys. **35**, 517 (1984).
[9]E. T. Gawlinski, M. Grant, J. D. Gunton, and K. Kaski, Phys. Rev. B **31**, 281 (1985).
[10]A. N. Burkitt and D. W. Heermann, Europhys. Lett. **10**, 207 (1989).
[11]C. Yeung, Phys. Rev. B **39**, 9652 (1989); A. Chakrabarti and J. D. Gunton, *ibid.* **37**, 9638 (1988).
[12]T. Ohta, D. Jasnow, and K. Kawasaki, Phys. Rev. Lett. **49**, 1223 (1982).
[13]J. Viñals and D. Jasnow, Phys. Rev. B **37**, 9582 (1988); H. Guo, Q. Zheng, and J. D. Gunton, *ibid.* **38**, 11 547 (1988).
[14]Y. Oono and S. Puri, Phys. Rev. Lett. **58**, 836 (1988); S. Puri and Y. Oono, Phys. Rev. A **38**, 1542 (1988).
[15]S. M. Allen and J. W. Cahn, Acta Metall. **27**, 1085 (1979); K. Kawasaki and T. Ohta, Prog. Theor. Phys. **67**, 147 (1982).
[16]Y. Oono and S. Puri, Mod. Phys. Lett. B **2**, 861 (1988).
[17]K. Kawasaki, M. C. Yalabik, and J. D. Gunton, Phys. Rev. A **17**, 455 (1978).
[18]M. T. Collins and H. C. Teh, Phys. Rev. Lett. **30**, 781 (1973); T. Hashimoto, T. Miyoshi, and M. Ohtsuka, Phy. Rev. B **13**, 1119 (1976).
[19]M. K. Phani, J. L. Lebowitz, and M. H. Kalos, Phys. Rev. Lett. **45**, 366 (1980); P. S. Sahni, G. Dee, J. D. Gunton, M. Phani, J. L. Lebowitz, and M. H. Kalos, Phys. Rev. B **24**, 410 (1981).
[20]G. Porod, in *Small Angle X-Ray Scattering,* edited by O. Glatter and L. Kratky (Academic, New York, 1983).
[21]M. Grant (private communication).
[22]An example in which Q is singular in the limit $\xi/L \to 0$ with $R(t)/L$ fixed is the local chemical potential $\mu(\mathbf{r},t)$. For the nonconserved order-parameter case, the local chemical potential is zero everywhere except at the interfaces where it is proportional to the local curvature. The probability distribution is of the form

$$P[\mu(\mathbf{r}),t,L,\xi]=(\xi/L)Q(\mu(\mathbf{r})L,l(t)/L)+\delta(\mu(\mathbf{r}))(1-c/L)\ .$$

The first term on the right-hand side is the scaling portion of P which is singular in the limit $\xi/L \to 0$ at fixed $R(t)/L$.
The first term on the right-hand side is the scaling portion of P which is singular in the limit $\xi/L \to 0$ at fixed $R(t)/L$.
[23]T. R. Rogers, and R. C. Desai, Phys. Rev. B **39**, 11 956 (1989); K. E. Elder, T. M. Rogers, and R. C. Desai, *ibid.* **38**, 4725 (1988).
[24]K. Kawasaki and T. Ohta, Physica A **118**, 175 (1983); K. Kawasaki, Ann. Phys. **154**, 319 (1984).
[25]H. A. Huse, Phys. Rev. B **34**, 7845 (1986).
[26]C. Roland and M. Grant, Phys. Rev. Lett. **60**, 2657 (1988); A. J. Bray, *ibid.* **62**, 2841 (1989); C. Roland and M. Grant, Phys. Rev. B **39**, 11 971 (1989).
[27]M. Grant and J. D. Gunton, Phys. Rev. B **28**, 5496 (1983); S. Puri and Y. Oono, J. Phys. A **21**, L755 (1988).